

Robust Heart Rate Variability and Interbeat Interval Detection Algorithm in the Presence of Motion Artifacts

Ayca Aygun³ and Roozbeh Jafari^{1,2,3}

Departments of Biomedical Engineering¹, Computer Science and Engineering², Electrical and Computer Engineering³
Texas A&M University, College Station, Texas, USA.
aycaaygun@tamu.edu, rjafari@tamu.edu

Abstract—This paper proposes a novel method to estimate heart rate variability (HRV) and interbeat interval (IBI) in the presence of motion artifacts. A robust heartbeat selection method is introduced as a shortest path exploration problem to detect HRV/IBI from a noisy signal. The time-continuity of heartbeats is used to model the shortest path. The end point of one heartbeat is the starting point of the next one. A graph is constructed whose vertices and edges are assumed to be the beginning of each possible heartbeats and the IBIs, respectively. Weights are assigned to the edges by using average heart rate (HR) values from state-of-the-art algorithms. The results indicate that IBI percentage error is around 3% for distorted ECG signal even with 0dB SNR. In addition, HRV parameters of clean versus noisy signals show high correlation.

Index Terms—Heart Rate Variability, Wearable Sensors, Physiological Signal Processing, Motion Artifacts

I. INTRODUCTION

Cardiovascular diseases (CVDs) are the leading cause of death globally, claiming more than 17.3 million lives per year [1], making cardiac fitness the most important indicator of physiological health. One of the most common sign of cardiac health is *average heart rate (HR)*, which is an average number of heart contractions per a fixed time period, normally over several heartbeats. Although, average HR is a well-studied indicator for cardiac exertion, the variations of HR may hold a significant information about the current status of heart due to its nonstationary nature [2]. *Heart rate variability (HRV)* is a physiological criterion of the variations between adjacent HRs, and can be obtained from *interbeat interval (IBI)*, which is a measure of HR for single heartbeat. Since, these fluctuations are related to different physiological conditions, HRV is a significant benchmark for monitoring the cardiovascular health. For instance, a scarce level of variations is an indicator of chronic stress besides an excessive level of variations is a sign of nervous system disorders [3]. Hence, HRV is an effective indicator for diagnosing underlying conditions such as cardiac inflammation, anxiety, stress, and poor sleep quality [3]–[5].

In wearable devices, HRV measurement becomes especially challenging due to motion artifacts caused by the movement of the user (*e.g.*, walking) or the sensor (*e.g.*, sliding, rubbing). Although, there are several noise reduction techniques in the literature for robust average HR measurement [6], [7]; noise reduction for HRV measurement is more challenging. Average HR is typically consistent and noise is not, hence it is easier to distinguish average HR from noise; while in the case of HRV, both noise and HRV offer inconsistency.

In this study, HRV and IBI are obtained from noisy ECG signals in the time domain that are distorted with motion artifacts. A robust peak selection method is introduced as a shortest path exploration problem to detect the HRV from a noisy signal. Graph theory is leveraged to represent heartbeats (R-peaks) as nodes and IBIs as edges. Particle Filtering is used to estimate the average HR and assign the weights to the edges [6] although any state-of-the-art technique can be used to measure the average HR such as Kalman filtering [7].

The main contributions of this work are:

- Development of an operator that can detect morphological features of interest across various physiological signals.
- Formalization of the morphological feature detection process as a shortest path exploration problem to realize the IBI estimation performance.
- Robust calculation of IBI and HRV parameters in the presence of motion artifacts.

II. RELATED WORKS

IBI detection is rather new and there are a small number of prior investigations in the literature that focus on detecting IBIs. One attempts to estimate the IBIs by using the characteristic locations of a radar signal. [8]. Although, this technique provides a way to obtain accurate IBIs, it requires an ultrawideband radar system which is not proper for further development in a wearable form factor. There have been a few techniques that provide an HRV estimation when there is no noise. One focuses on the measurement of HRV using off-the-shelf smart phones [9]. Although this method provides satisfying accuracy rates of HRV for static subjects, it does not provide a technique to obtain the HRV parameters from noisy signals. Another investigation introduces a technique to extract the HRV values from Smartphone PPG [10]. Again, this technique requires steady subjects to obtain the HRV parameters accurately which is not practical in daily life.

There have been several techniques to detect average HR which is essential also for our algorithm. While techniques such as Kalman filtering [7] and particle filtering [6] take into account randomized noise for distorted signals, they are used for calculation of average HR. Since HRV includes variability, it requires additional processing beyond filtering techniques used for average HR.

III. METHOD

This work introduces a robust IBI and HRV detection algorithm in the presence of motion artifacts. The proposed

method is applicable to different signal modalities which is explained in the following section in detail.

A. Physiological Signal Modalities

There are various physiological signal modalities represented in Fig. 1, all of them have different characteristics such as the foot of a bio-impedance (Bio-Z) signal, R-peak of an ECG signal, and maximum slope or systolic peak of a PPG signal.

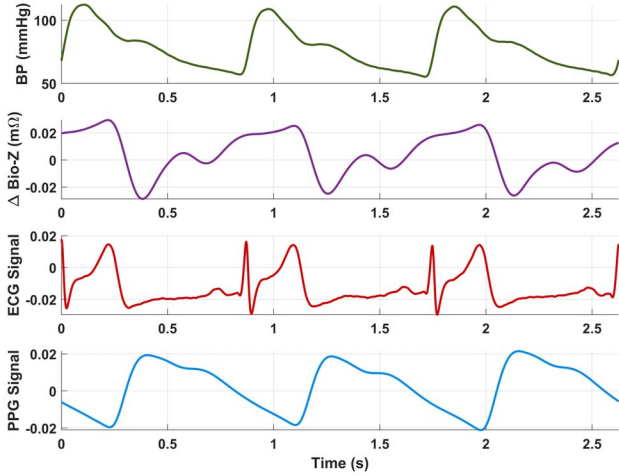


Fig. 1: Different Physiological Signal Modalities to Monitor the Cardiac Activity [11].

This work explores the detection of R-peaks and IBIs in a noisy ECG signal to estimate the IBI/HRV. The R-peaks are estimated with the help of the sequential alignments of IBIs in time domain and the strength of R-peaks. IBI for ECG is the time difference between two consecutive R-peaks. Fig. 2 represents two R-peaks of an ECG signal and an IBI between them.

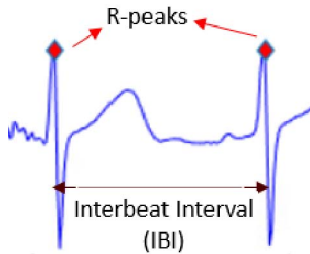


Fig. 2: ECG Signal showing two R-peaks and an IBI.

B. Observation Mechanism

The flowchart of our proposed IBI/HRV detection algorithm is presented in Fig. 3. First, the noisy signal is passed through a number of static filters to remove the out of band noise. In this work, a noisy ECG signal is preprocessed to remove the out-of-band noise with a high pass filter (HPF) with 0.5Hz cutoff frequency and continuous wavelet transform (CWT)

with the Mexican hat wavelet by applying a center frequency of 0.25Hz suggested in the previous work [6]. Next, a feature detection operator is used to detect the morphological features of the signal. For the current work, the morphological feature detection operator is used to obtain all possible choices of R-peaks as a significant signal characteristic of an ECG signal and these R-peaks are used inside the shortest path calculation. Since this mechanism is signal-agnostic, it can be used for various signal modalities, such as the maximum slope or the systolic peak detection of a PPG waveform instead of R-peak for an ECG signal. Finally, a graph model is constructed and a shortest path is calculated that denotes the most likely sequence of heartbeats (R-peaks for ECG) in the presence of the remaining in-band noise.

C. Shortest Path Calculation

A graph is constructed where the vertices represent candidate R-peaks, and the edges represent IBIs. The weights of the edges are a function of the average IBI calculated from the average HR. In the time domain, R-peaks are sequentially aligned with no discontinuity between them, *i.e.*, the ending R-peak of a certain IBI is the starting R-peak of the subsequent IBI. Then, a shortest path calculation is used for the detection of the R-peaks. Fig. 4 shows a schematic for the shortest path calculation. A particle filter approach is used to calculate average HR [6], which is then used for calculating the IBI as:

$$IBI_{avg} = \frac{60000}{HR_{avg}} [ms] \quad (1)$$

To provide an illustrative example, at the top of the Fig. 4, the peaks of the noisy ECG and the true R-peaks of the clean ECG are indicated with green and red signs, respectively. The vertices (candidate R-peaks) are indicated as v_1, v_2, \dots, v_N where N is the number of vertices. The time difference between two vertices, v_i and v_j , is represented as the edge e_{ij} . We have color coded the edges to demonstrate how our technique works. All edges are defined either as possible edge (green) or as unlikely edge (red) by means of their weights, seen at the bottom of the Fig. 4. We need to determine proper weights to the edges to capture this property. After the weights are assigned to the edges, the path with the smallest cost is likely the best set of R-peaks. The caveat is to design the weights so the most likely edges for representing the most likely R-peaks will be selected for the final shortest path. In the following, we explain how the edge weights are constructed.

In this work, we obtain the average HR/IBI using particle filtering technique for 8-sec windows, that are centered around the candidate R-peaks. For any 8-sec time window, the minimum and maximum IBI values are defined as follows:

$$(IBI_{min})_i = (IBI_{avg})_i - \varepsilon \quad (2)$$

$$(IBI_{max})_i = (IBI_{avg})_i + \varepsilon \quad (3)$$

In this work, the ε is chosen as 0.05 seconds empirically to obtain the $(IBI_{min})_i$ and $(IBI_{max})_i$ values dynamically for

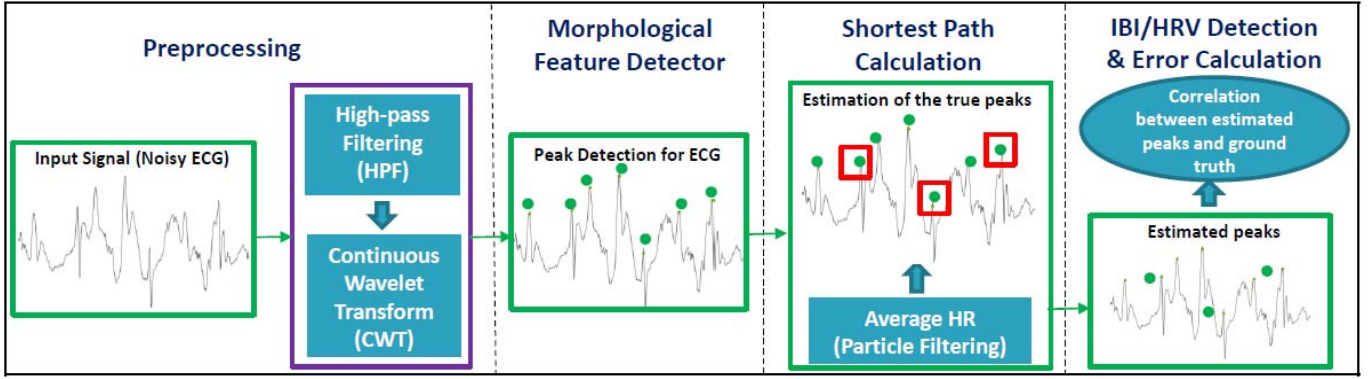


Fig. 3: Flowchart of the IBI/HRV Detection Algorithm

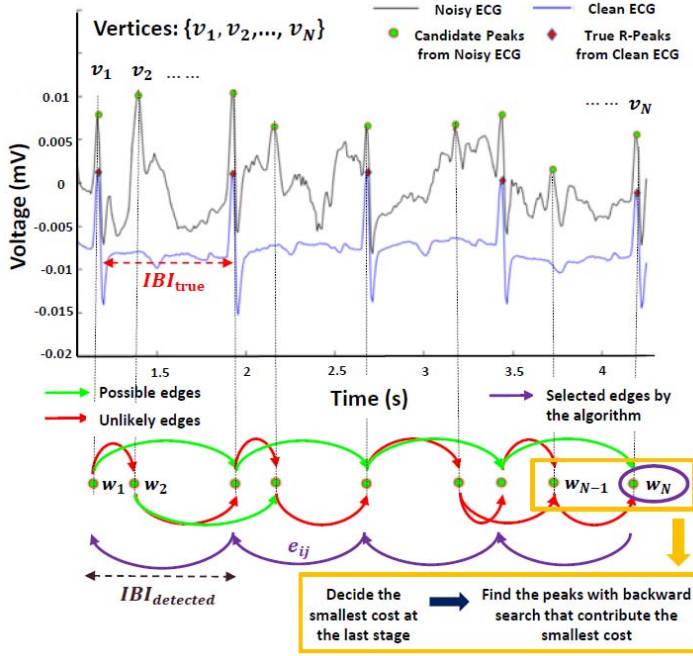


Fig. 4: Shortest Path Modeling and Node Detection

each vertex. Finally, the weight for an edge e_{ij} is represented by w_{ij} , such that:

$$w_{ij} = e^{\min(|(IBI_{min})_i - e_{ij}|, |(IBI_{max})_i - e_{ij}|)} \quad (4)$$

If e_{ij} lies within the range $(IBI_{min})_i$ and $(IBI_{max})_i$, it is assigned a weight of zero.

The exponential function increases the penalization when the distance between any pair of vertices is not between $(IBI_{min})_i$ and $(IBI_{max})_i$ thresholds, penalizing unlikely R-peaks. Considering each new R-peak starts when the previous R-peak ends, this problem reduces to finding a possible path connecting the first R-peak to the last R-peak. The path with least cost selects the most likely R-peaks closer to average IBI. The details are presented in Algorithm 1.

Algorithm 1 Shortest Path Modeling, Cost Assignment and Shortest Path Detection

◆ Calculate the weights:
for $i = 2$ to N **do**
 for $j = i - m_i$ to $i - 1$ **do**
 Calculate w_{ij}
 end for
 $w_i = \min(w_{ij} + w_j)$
 $pn_{v_i} = \arg \min_{v_j \in C_i} (w_{ij} + w_j)$
end for

where m_i is the number of former neighbors of v_i ($m_i < i$) and pn_i is the chosen previous node for v_i that contributes minimum accumulated cost to the candidate node v_i .

◆ Decide the minimum accumulated distance in the last time interval $(t_{min})_N$. The last node set:

$$P_N = (v_{N-m_N}, \dots, v_{N-1}, v_N)$$

The smallest accumulated distance is decided as below:

$$v_{chosen} = \arg \min_{v_k} ((w_N, w_{N-1}, \dots, w_{N-m_N}) \text{ where } k = N - m_N, \dots, N - 1, N.$$

$$V_{chosen} = v_{chosen}$$

where v_{chosen} is the chosen last vertex and V_{chosen} is the set of all chosen vertices.

◆ Backward search:

for $k = N$ to 1 **do**
 if $v_{chosen} == v_k$ **then**
 $v_k = pn_k$
 end if
 $V_{chosen} = (V_{chosen}, v_k)$
end for

IV. EXPERIMENTAL RESULTS

A. Experimental Setup

ECG signals, corrupted with real motion artifact noise, are used from the MIT-BIH Noise Stress Test Database to test the performance of our algorithm [12], [13]. Three signal distortion levels are used: 6dB, 3dB, and 0dB. The clean reference ECG signals are taken from the IEEE Signal Processing Cup 2015 (SP Cup) database [14].

TABLE I: IBI Percentage Errors for Different SNR Levels

Subjects SNR Level	1	2	3	4	5	6	7	8	9	10	11	12	Average
6dB	0.87	0.55	0.53	0.37	0.34	2.08	3.39	0.39	0.54	0.53	2.61	0.62	1.07%
3dB	1.77	1.36	1.01	0.85	1.18	3.44	2.23	1.09	1.16	0.71	2.87	1.55	1.60%
0dB	3.06	3.84	2.74	1.72	2.86	2.85	3.96	4.39	3.60	1.83	4.11	3.93	3.25%

The IBI percentage errors are calculated by using the estimated IBIs from noisy ECG and the true IBIs obtained from the clean reference ECG with the equation as follows:

$$IBI_{err} = \frac{1}{n} \sum_{i=1}^n \left[\frac{|t_i - t'_i| + |t_{i+1} - t'_{i+1}|}{|t_i - t_{i+1}|} \times 100 \right] \quad (5)$$

where n is the number of IBIs, t_i 's are true R-peaks from the clean reference ECG signal and t'_i 's are the estimated R-peaks from the noisy ECG signal.

The estimated IBIs are used as inputs into the Kubios software for obtaining the HRV parameters [15]. Then, the correlations between the HRV results from the reference non-noisy signals and the HRV results from the noise-induced signals are calculated. Six different HRV parameters are chosen: the mean IBI (ms), the SDNN (standard deviation of IBI in ms), the mean HR ($1/min$), the STD HR (standard deviation of HR in $1/min$), the VLF power (very low frequency power in ms^2), and the total power (ms^2).

B. Results and Discussions

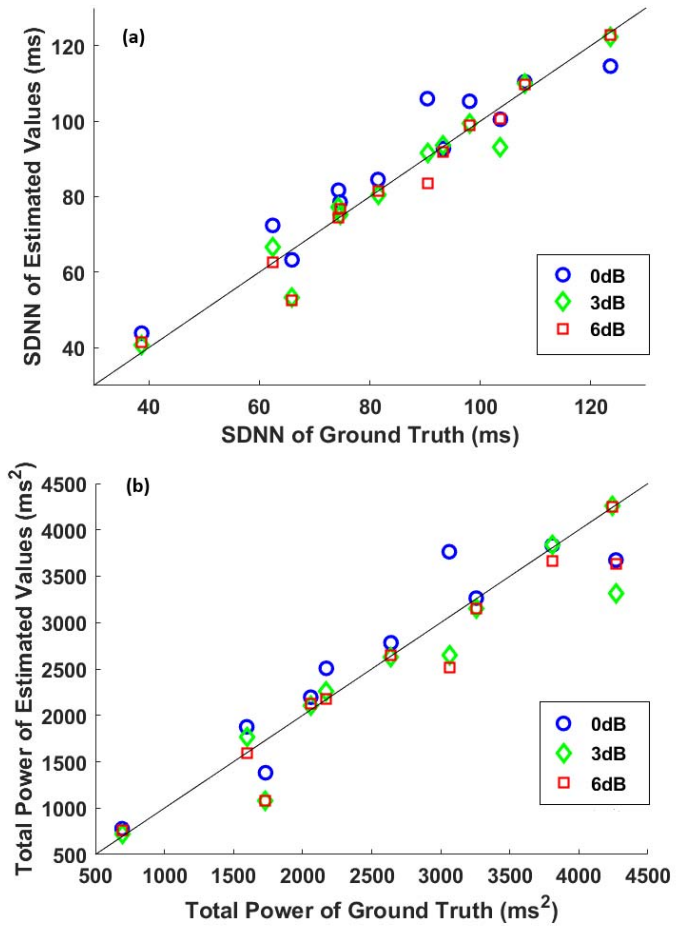
Table I shows the IBI percentage errors for 12 different subjects at three different noise levels. The errors are 1.07%, 1.60%, and 3.25% for the SNR values of 6dB, 3dB, and 0dB, respectively. The results show that the proposed method provides a good accuracy for detecting IBI even when the signal strength is highly corrupted at 0dB SNR. The correlations of the six HRV parameters between the results from the clean ECG and the estimated results from the noisy ECG corrupted by different SNR values are represented in Table II, which hover around 0.96. The results indicate that the true values and the estimations are highly correlated even with 0dB SNR.

TABLE II: Correlation of HRV Parameters Between Ground Truth and Obtained Results for Different SNR Levels

SNR Level	6dB	3dB	0dB
HRV Parameter			
Mean IBI	0.9960 (p<0.001)	0.9955 (p<0.001)	0.9956 (p<0.001)
STD RR (SDNN)	0.9814 (p<0.001)	0.9740 (p<0.001)	0.9598 (p<0.001)
Mean HR	0.9960 (p<0.001)	0.9957 (p<0.001)	0.9958 (p<0.001)
STD HR	0.9297 (p<0.001)	0.9478 (p<0.001)	0.8995 (p<0.001)
VLF Power	0.8981 (p<0.001)	0.8995 (p<0.001)	0.9293 (p<0.001)
Total Power	0.9569 (p<0.001)	0.9533 (p<0.001)	0.9588 (p<0.001)

Fig. 5 shows the correlation plots of two different HRV parameters (SDNN and Total Power) between the results from the clean ECG and the estimated results from the noisy ECG corrupted by different SNR values. The HRV parameters are

obtained from 12 subjects individually and for three SNR levels. We observed high correlation even with 0dB SNR.


 Fig. 5: Correlation Plots of HRV Parameters: (a) SDNN (ms), (b) Total Power (ms^2).

V. CONCLUSION

In this work, a shortest path algorithm is used to detect R-peaks from a noisy ECG signal for the robust estimation of IBI and HRV. Our experimental results indicate a low average IBI error of around 3% and high correlation of HRV parameters even for signals highly corrupted with motion artifact noise. A morphological feature detection operator is used to leverage the signal characteristics of an ECG signal. Moreover, this operator can be applied to different sensor modalities for future work such as PPG and Bio-Z for similar motion artifact rejection techniques. Additionally, this algorithm is particularly

beneficial for enabling reliable and accurate prediction of HRV and IBI using wearable devices.

VI. ACKNOWLEDGMENT

This work was supported, in part, by funding from the National Science Foundation Engineering Research Center for Precise Advanced Technologies and Health Systems for Underserved Populations (PATHS-UP) (EEC-1648451). Any opinions, findings, conclusions, or recommendations expressed in this material are those of the authors and do not necessarily reflect the views of the funding organizations.

REFERENCES

- [1] F. Peter Libby, MD, Robert O. Bonow, MD, Douglas P. Zipes, MD and Douglas L. Mann, MD, *Braunwald's Heart Disease: A Textbook of Cardiovascular Medicine*, 8th ed. 2007.
- [2] U. R. Acharya, K. P. Joseph, N. Kannathal, C. M. Lim, and J. S. Suri, "Heart rate variability: A review," *Medical and Biological Engineering and Computing*, 2006.
- [3] R. McCraty and F. Shaffer, "Heart rate variability: New perspectives on physiological mechanisms, assessment of self-regulatory capacity, and health risk," 2015.
- [4] H. Cohen and J. Benjamin, "Power spectrum analysis and cardiovascular morbidity in anxiety disorders," 2006.
- [5] J. Parak, A. Tarniceriu, P. Renevey, M. Bertschi, R. Delgado-Gonzalo, and I. Korhonen, "Evaluation of the beat-to-beat detection accuracy of PulseOn wearable optical heart rate monitor," in *Proceedings of the Annual International Conference of the IEEE Engineering in Medicine and Biology Society, EMBS*, 2015.
- [6] V. Nathan, I. Akkaya, and R. Jafari, "A particle filter framework for the estimation of heart rate from ECG signals corrupted by motion artifacts," in *Proceedings of the Annual International Conference of the IEEE Engineering in Medicine and Biology Society, EMBS*, 2015.
- [7] K. T. Sweeney, T. E. Ward, and S. F. McLoone, "Artifact removal in physiological signals-practices and possibilities," *IEEE Transactions on Information Technology in Biomedicine*, 2012.
- [8] T. Sakamoto, R. Imasaka, H. Taki, T. Sato, M. Yoshioka, K. Inoue, T. Fukuda, and H. Sakai, "Feature-based correlation and topological similarity for interbeat interval estimation using ultrawideband radar," *IEEE Transactions on Biomedical Engineering*, 2016.
- [9] R. Y. Huang and L. R. Dung, "Measurement of heart rate variability using off-the-shelf smart phones," *BioMedical Engineering Online*, 2016.
- [10] R. C. Peng, X. L. Zhou, W. H. Lin, and Y. T. Zhang, "Extraction of heart rate variability from smartphone photoplethysmograms," *Computational and Mathematical Methods in Medicine*, 2015.
- [11] B. Ibrahim and R. Jafari, "Continuous Blood Pressure Monitoring using Wrist-worn Bio-impedance Sensors with Wet Electrodes," in *2018 IEEE Biomedical Circuits and Systems Conference, BioCAS 2018 - Proceedings*, 2018.
- [12] A. L. Goldberger, L. A. Amaral, L. Glass, J. M. Hausdorff, P. C. Ivanov, R. G. Mark, J. E. Mietus, G. B. Moody, C. K. Peng, and H. E. Stanley, "PhysioBank, PhysioToolkit, and PhysioNet: components of a new research resource for complex physiologic signals.," *Circulation*, 2000.
- [13] G. Moody, W. Muldrow, and R. Mark, "The MIT-BIH Noise Stress Test Database," in *Computers in Cardiology*, 1984.
- [14] Z. Zhang, Z. Pi, and B. Liu, "TROIKA: A general framework for heart rate monitoring using wrist-type photoplethysmographic signals during intensive physical exercise," *IEEE Transactions on Biomedical Engineering*, 2015.
- [15] M. P. Tarvainen, J. P. Niskanen, J. A. Lipponen, P. O. Ranta-aho, and P. A. Karjalainen, "Kubios HRV - Heart rate variability analysis software," *Computer Methods and Programs in Biomedicine*, 2014.